Atmos. Meas. Tech. Discuss., 7, 7701–7715, 2014
www.atmos-meas-tech-discuss.net/7/7701/2014/
doi:10.5194/amtd-7-7701-2014
© Author(s) 2014. CC Attribution 3.0 License.

Atmospheric Measurement Techniques Discussions
Open Access

This discussion paper is/has been under review for the journal Atmospheric Measurement Techniques (AMT). Please refer to the corresponding final paper in AMT if available.

Characterization of model errors in the calculation of tangent heights for atmospheric infrared limb measurements

M. Ridolfi[1,2] **and L. Sgheri**[3]

[1]Dipartimento di Fisica e Astronomia, Università di Bologna, Italy
[2]Istituto di Fisica Applicata "Carrara", Consiglio Nazionale delle Ricerche, Firenze, Italy
[3]Istituto per le Applicazioni del Calcolo, Consiglio Nazionale delle Ricerche, Firenze, Italy

Received: 13 May 2014 – Accepted: 8 July 2014 – Published: 28 July 2014

Correspondence to: L. Sgheri (l.sgheri@iac.cnr.it)

Published by Copernicus Publications on behalf of the European Geosciences Union.

Abstract

We review the main factors driving the calculation of the tangent height of spaceborne limb measurements: the ray-tracing method, the refractive index model and the assumed atmosphere. We find that commonly used ray-tracing and refraction models are very accurate, at least in the middle-infrared. The factor with largest effect in the tangent height calculation is the assumed atmosphere. Using a climatological model in place of the real atmosphere may cause tangent height errors up to ±200 m. Depending on the adopted retrieval scheme, these errors may have a significant impact on the derived profiles.

1 Introduction

Accurate knowledge of the instrument line of sight is essential to properly geolocate the profile values inferred from atmospheric limb emission measurements acquired from space. Spectral measurements contain also information on the instrument viewing direction, however the spectral resolution and the signal-to-noise ratio are often insufficient to determine, accurate estimates of the line of sight. Therefore, retrieval codes benefit from accurate a-priori knowledge of the tangent height of the analyzed limb measurements (Ridolfi et al., 2000; Raspollini et al., 2006; Dudhia et al., 2005; Raspollini et al., 2013). The calculation of accurate tangent heights from the engineering estimates of the instrument pointing angles and instrument position relies, however, on the accuracy both of the ray tracing algorithm and of the model used for atmospheric refraction. In this work we compare the accuracy of a few ray tracing and atmospheric refraction models applicable to mid-infrared limb measurements. The tests presented are based on measurements of the Michelson Interferometer for Passive Atmospheric Sounding (MIPAS) that successfully operated on board of the polar satellite ENVISAT in the time frame from April 2002 to April 2012 (Fischer et al., 2008).

AMTD
7, 7701–7715, 2014

2 Ray-tracing

The propagation path of electromagnetic rays through an inhomogeneous medium can be deduced from the Eikonal equation (Born and Wolf, 1970):

$$|\nabla\phi(\boldsymbol{x})|^2 = n^2(\boldsymbol{x}). \tag{1}$$

where $\boldsymbol{x}$ is the position vector, $n(\boldsymbol{x})$ the refractive index and $\phi(\boldsymbol{x})$ is the so called *Eikonal function*. This equation can be derived directly from the first-order Maxwell equations or from the second-order wave equations for either the electric or the magnetic field. The only simplifying assumption used in this derivation is that $n(\boldsymbol{x})$ varies slowly with respect to the wavelength of the electromagnetic field. Of course, for propagation of mid-infrared radiation in the Earth's atmosphere this hypothesis is verified with very high accuracy. The surfaces $\phi(\boldsymbol{x})$ = constant are the geometrical wave-fronts. Therefore, the ray direction is parallel to $\nabla\phi(\boldsymbol{x})$. Let $\boldsymbol{p}(s)$ be the ray path, parametrized with the arc parameter s. We can write:

$$\frac{\mathrm{d}\boldsymbol{p}(s)}{\mathrm{d}s} = \frac{\nabla\phi(\boldsymbol{p}(s))}{|\nabla\phi(\boldsymbol{p}(s))|} \tag{2}$$

After some algebraic manipulations, using Eq. (1) we get the differential form of the light rays equation (Born and Wolf, 1970):

$$\frac{\mathrm{d}}{\mathrm{d}s}\left(n(\boldsymbol{p}(s))\frac{\mathrm{d}\boldsymbol{p}(s)}{\mathrm{d}s}\right) = \nabla n(\boldsymbol{p}(s)). \tag{3}$$

This is a vectorial second-order differential equation that permits to derive the full ray path across an inhomogeneous medium, if $n(\boldsymbol{x})$ and the boundary conditions are known. From this equation, several ray-tracing methods can be derived with different trade-off between accuracy and computational speed. In this work we consider the following three ray-tracing methods:

AMTD
7, 7701–7715, 2014

– direct numerical solution of Eq. (3),

– tangential displacement method (Stiller, 2000),

– iterative Snell's law of Thayer (Thayer, 1967; Hobiger et al., 2008).

While the iterative Snell's law is one of the fastest ray-tracing methods, it relies on the hypothesis of a horizontally homogeneous refractive index. However, if the horizontal variability of the atmosphere is taken into account, this method is not adequate. For horizontally varying atmosphere, the level lines of $n(\boldsymbol{x})$ do not coincide with the altitude levels. Thus the calculation of the refraction angle with the Snell's law is based on a wrong hypothesis. In our tests we found that in several synthetic but realistic atmospheric conditions, with strong horizontal gradients of pressure and temperature, the method produces a wrong ray-path, partly following Earth's curvature. In Hobiger et al. (2008) a refined approach of Thayer's method is proposed at the expense of a significantly increased computational complexity.

The tangential displacement method (henceforth referred to as TD) is an iterative approach for the solution of the Eikonal equation, using an approximation to avoid the calculation of the second derivatives of $\boldsymbol{p}(s)$.

For the direct numerical solution of the Eikonal equation we implemented a multi-step predictor-corrector method (henceforth referred to as EIK) using the two-step Adams–Bashforth formula for the predictor and the BDF2 formula for the corrector (Isaacson, 1994). The shape of the ray path, however, suggests the use of an adaptive step length based on the second derivatives of $\boldsymbol{p}(s)$ that are linked to the ray local curvature. These derivatives are easily obtained from the numerical solution of the Eikonal equation. Thus we also implemented this adaptive method (henceforth referred to as AEIK) still maintaining the property that in each atmospheric layer the step is fixed. This is an efficient choice in view of the implementation of the Curtis–Godson integrals for the calculation of the radiative transfer in a horizontally varying atmosphere.

All the implemented methods can be applied to a three-dimensional ray-tracing. Our implementation is however planned for inclusion in the ESA retrieval model for MIPAS

AMTD
7, 7701–7715, 2014

routine data processing (Ridolfi et al., 2000; Raspollini et al., 2006, 2013), which assumes that all limb scans lie in the orbit plane. In a forthcoming evolution of this algorithm the atmosphere will be represented with a 2-D discretization in the orbit plane and will be considered constant in the direction perpendicular to this plane. Under this assumption all the ray-paths lie in this plane, therefore we implemented a 2-D ray-tracing scheme.

3 Atmospheric refraction model

In this work we considered three refractive index models:

- Barrell–Sears formula (Barrel and Sears, 1939),
- simplified Edlén's formula (Edlén, 1966),
- Ciddor's formula (Ciddor, 1996).

A good on-line comparison of refraction formulas can be found in Young (2011).

The Barrel–Sears empirical formula has been used for long time also for atmospheric infrared applications. We include in our tests this formula mainly for historical reasons. The version implemented in our code is:

$$(n-1)\times 10^6 = \left(77.48 + \frac{0.44}{\lambda^2} + \frac{0.007}{\lambda^4}\right)\frac{p}{T} - \left(12.79 - \frac{0.14}{\lambda^2}\right)\frac{p_w}{T}. \quad (4)$$

where p is the total air pressure expressed in hPa, T is the temperature in Kelvin, λ the wavelength in µm and p_w is the water vapor partial pressure in hPa.

The simplified Edlén's formula is the model currently implemented in the ESA retrieval code for routine MIPAS data inversion. The formula implemented in our code is:

$$n - 1 = c_0 \cdot \frac{T_0}{p_0} \cdot \frac{p}{T} \quad (5)$$

AMTD
7, 7701–7715, 2014

with the constants $p_0 = 1013.25\,\text{hPa}$, $T_0 = 288.16\,\text{K}$, and $c_0 = 0.000272632$. This formula clearly does not model the dependence of the refraction on the wavelength and the water vapor amount.

Ciddor's formula models the refractive index as a function of wavelength, pressure, temperature, water vapor and carbon dioxide content. The formula was originally tested with experimental data extending only up to 1.7 µm, however the work of Mathar (2004) suggests that its accuracy is of the order of $1/10^6$ also up to 25 µm, i.e. over the whole spectral region covered by MIPAS observations (4.1–14.9 µm). We implemented Ciddor's formula following the original paper (Ciddor, 1996).

4 Atmospheric models

Whatever refraction model is chosen, the refractivity depends on pressure, temperature and, possibly, water vapor and carbon dioxide. Thus the ray-tracing depends on the assumed atmosphere. To evaluate the impact of the selected atmosphere we considered the following models:

- the US Standard Atmosphere, 1976 (US Gov., 1976),
- the IG2 atmosphere (Remedios et al., 2007),
- the atmosphere retrieved in a previous processing version of MIPAS data (Raspollini et al., 2013),
- atmospheric refractivity profiles determined from co-located Radio Occultation (RO) measurements (Schwärz et al., 2012).

The US Standard Atmosphere (US76), together with the simplified Edlén's formula for refraction is the model currently adopted by ESA in MIPAS Level 1b data processing (Kleinert et al., 2007) to determine the tangent height of the limb measurements, starting from the instrument position and pointing angles. The US76 atmosphere does not include any model for the horizontal or seasonal variabilities.

AMTD
7, 7701–7715, 2014

The so called "IG2" is a climatological database of atmospheres developed for use as Initial Guess (IG) or assumed profiles in MIPAS routine Level 2 retrievals (Remedios et al., 2007). The IG2 database includes vertical profiles of pressure, temperature and Volume Mixing Ratio (VMR) of constituents relevant for MIPAS data processing. The profiles are tabulated as a function of year, season and latitude band. In our tests we also linearly interpolate the profiles in latitude, in between the tabulated values. This interpolation makes the atmosphere smoothly changing with latitude, avoiding abrupt changes at the edges of the latitude bands.

The last two atmospheres rely on experimental data. The tests with RO refractivity measurements considered in this work are limited to the MIPAS orbit 43442 acquired on 21 June 2010. In this orbit there are 16 MIPAS limb scans for which a co-located RO measurement exists within 300 km and 3 h.

5 Results

The calculated ray-path depends on: the ray-tracing method, the refractive index model and the assumed atmosphere. To evaluate the impact of each of these factors on the calculated tangent height of the limb measurements we use the following approach. The MIPAS Level 1b data files provide the geolocation of the tangent points of the limb measurements. These are determined using the position and attitude of the satellite via a ray-tracing algorithm that uses the US76 atmosphere and the simplified Edlén's formula for refractivity. Starting from these tangent points we use the same assumptions of the Level 1b processor to back-calculate the latitude and the slope of the ray-path at the intersection of the atmospheric boundary, fixed at 120 km (outgoing path). Then we reverse the ray-tracing (incoming path) and recalculate the tangent point, possibly using different assumptions. The difference in height between the original and the re-calculated tangent point characterizes the impact of the different assumptions used for the incoming path.

AMTD
7, 7701–7715, 2014

First we tested the accuracy and the computational efficiency of the ray-tracing methods described in Sect. 2. For each limb measurement we calculated the incoming path using the same assumptions of the outgoing path. The difference in height between the original and the recalculated tangent point represents, in this case, the numerical error introduced by the ray-tracing algorithm. To quantify the overall accuracy of the tested methods, we use the summation of the absolute values of these errors in the whole orbit. The accuracy depends on the step-length used by the ray-tracing. The smaller the step-length used the more accurate is the solution, however smaller step-lengths require longer computing time.

In Fig. 1 we show the trade-off between accuracy and computing time for the different methods described, for various step-lengths. In the case of the AEIK method the values reported in the figure are the initial step-lengths, which are then adapted by the method itself. For sufficiently small step-lengths all the three considered methods are very accurate. The AEIK method is the most efficient, it however requires a more elaborated code. In our subsequent tests we use the AEIK method.

With fixed US76 atmosphere, we then tested the impact of the refractive index model used for the incoming path. Differences between original and recalculated tangent heights are always much smaller than the accuracy required for tangent heights (50–100 m). The Simplified Edlén's and Ciddor's formulas turn out to be in very good agreement, providing differences in tangent heights less than 21 cm. The old Barrell–Sears formula provides slightly more differing results compared to the other two refraction models (within 2.3 m). In our subsequent tests we use the Ciddor's formula that we consider the most accurate.

Finally, with the same strategy we studied the impact of the assumed atmosphere on the ray-tracing. As expected, we found that this is the assumption with the largest impact on the calculation of the height of the tangent points. In Fig. 2 we show the differences (color scale) in meters between the original and recalculated tangent heights, as a function of the orbital coordinate (horizontal axis) and height (vertical axis). We only show tangent heights less than 20 km, since for higher tangent heights the difference

AMTD
7, 7701–7715, 2014

is less than 10 m. In Fig. 2a the assumed atmosphere for the incoming path is the IG2 atmosphere, in Fig. 2b the retrieved atmosphere. We note that above the troposphere the two panels show a good agreement. In the troposphere, where the atmospheric variability is larger, there are some differences. The larger differences are observed for the retrieved atmosphere and the lowest tangent heights where values up to 200 m are achieved. We do not show the results of the RO data, since they concern only 16 limb scans and the results are very similar to those obtained with the retrieved atmosphere, see Fig. 2b.

In order to assess the influence of the newly calculated tangent heights on the Level 2 products, we retrieved orbit 43442 starting from the recalculated tangent heights using the ESA operational algorithm (Ridolfi et al., 2000; Raspollini et al., 2006, 2013). On average the differences in the retrieved profiles are much smaller than the noise error, with no real improvement in the final χ^2 of the fit. However, locally, in the scans with large height corrections, the differences can be of the order of the noise error.

The small size of the differences in the retrieved profiles is due to the ability of the ESA retrieval code to adjust the pressure at the tangent points and recalculate tangent height increments using the hydrostatic equilibrium. To prove this assertion we forced the retrieval program to keep constant the tangent pressure during the iterations. In this case the retrieved profiles are more sensitive to the used tangent height values. In Fig. 3 we show the influence on the temperature profile, retrieved using the original (T_{L1b}) and recalculated (T_{RET}) tangent heights. Fig. 3a refers to the standard ESA retrieval algorithm, while in Fig. 3b we impose a constant tangent pressure. In both plots the average profile of $T_{\mathrm{RET}} - T_{\mathrm{L1b}}$ is shown (blue curve), together with its standard deviation (gold curve), and the average noise error of the T_{RET} (magenta curve) and T_{L1b} (red curve) profiles. The magenta and red curves in both panels are almost identical. Note that both the average difference and the standard deviation are larger in Fig. 3b. At the lowest altitudes there are significant values of $T_{\mathrm{RET}} - T_{\mathrm{L1b}}$, with differences as large as 5 K, correlated with the largest tangent height corrections plotted in Fig. 2b. Since the tangent pressure is kept fixed in the retrieval of Fig. 3b, the algorithm can not

AMTD
7, 7701–7715, 2014

use this parameter to adjust the tangent heights. Therefore temperature is used, via hydrostatic equilibrium, to compensate for the error in tangent heights.

6 Conclusions

We analyzed the main factors driving the calculation of the tangent heights of space-borne limb measurements. We found that the factor with largest effect in the tangent height calculation is the assumed atmosphere. Using a climatological model in place of the real atmosphere may cause tangent height errors up to ±200 m. In MIPAS retrievals this inaccuracy causes a temperature error of the order of the noise error, if the tangent height is adjusted by fitting the tangent pressure (this is the case of the ESA algorithm). However, if the retrieval assumes a fixed tangent pressure, the inaccuracies in tangent heights may cause temperature differences locally exceeding 4–5 K.

Acknowledgements. This study was supported by the ESA-ESRIN contract 21719/08/I-OL.

References

Barrell, H. and Sears, J. E.: The refraction and dispersion of air for the visible spectrum, Philos. T. R. Soc. A, 238, 1–62, 1939. 7705

Born, M. and Wolf, E.: Principles of Optics, 4th edn., Pergamon Press, 1970. 7703

Ciddor, P. E.: Refractive index of air: new equations for the visible and near infrared, Appl. Optics, 35, 1566–1573, 1996. 7705, 7706

Dudhia, A., Jay, V. L., and Rodgers, C. D.: MIPAS Orbital Retrieval using Sequential Estimation, available at: http://www.atm.ox.ac.uk/MORSE/ (last access: 24 July 2014), 2005. 7702

Edlén, B.: The refractive index of air, Metrologia, 2, 71–80, 1966. 7705

Fischer, H., Birk, M., Blom, C., Carli, B., Carlotti, M., von Clarmann, T., Delbouille, L., Dudhia, A., Ehhalt, D., Endemann, M., Flaud, J. M., Gessner, R., Kleinert, A., Koopman, R., Langen, J., López-Puertas, M., Mosner, P., Nett, H., Oelhaf, H., Perron, G., Remedios, J., Ridolfi, M., Stiller, G., and Zander, R.: MIPAS: an instrument for atmospheric and climate research, Atmos. Chem. Phys., 8, 2151–2188, doi:10.5194/acp-8-2151-2008, 2008. 7702

AMTD
7, 7701–7715, 2014

Hobiger, T., Ichikawa, R., Koyama, Y., and Kondo, T.: Fast and accurate ray-tracing algorithms for real-time space geodetic applications using numerical weather models, J. Geophys. Res., 113, D20302, doi:10.1029/2008JD010503, 2008. 7704

Isaacson, E.: Analysis of Numerical Methods, Courier Dover Publications, 1994. 7704

Kleinert, A., Aubertin, G., Perron, G., Birk, M., Wagner, G., Hase, F., Nett, H., and Poulin, R.: MIPAS Level 1B algorithms overview: operational processing and characterization, Atmos. Chem. Phys., 7, 1395–1406, doi:10.5194/acp-7-1395-2007, 2007. 7706

Mathar, R. J.: Calculated refractivity of water vapor and moist air in the atmospheric window at 10 µm, Appl. Optics, 43, 928–932, 2004. 7706

Raspollini, P., Belotti, C., Burgess, A., Carli, B., Carlotti, M., Ceccherini, S., Dinelli, B. M., Dudhia, A., Flaud, J.-M., Funke, B., Höpfner, M., López-Puertas, M., Payne, V., Piccolo, C., Remedios, J. J., Ridolfi, M., and Spang, R.: MIPAS level 2 operational analysis, Atmos. Chem. Phys., 6, 5605–5630, doi:10.5194/acp-6-5605-2006, 2006. 7702, 7705, 7709

Raspollini, P., Carli, B., Carlotti, M., Ceccherini, S., Dehn, A., Dinelli, B. M., Dudhia, A., Flaud, J.-M., López-Puertas, M., Niro, F., Remedios, J. J., Ridolfi, M., Sembhi, H., Sgheri, L., and von Clarmann, T.: Ten years of MIPAS measurements with ESA Level 2 processor V6 – Part 1: Retrieval algorithm and diagnostics of the products, Atmos. Meas. Tech., 6, 2419–2439, doi:10.5194/amt-6-2419-2013, 2013. 7702, 7705, 7706, 7709

Remedios, J. J., Leigh, R. J., Waterfall, A. M., Moore, D. P., Sembhi, H., Parkes, I., Greenhough, J., Chipperfield, M.P., and Hauglustaine, D.: MIPAS reference atmospheres and comparisons to V4.61/V4.62 MIPAS level 2 geophysical data sets, Atmos. Chem. Phys. Discuss., 7, 9973–10017, doi:10.5194/acpd-7-9973-2007, 2007. 7706, 7707

Ridolfi, M., Carli, B., Carlotti, M., von Clarmann, T., Dinelli, B. M., Dudhia, A., Flaud, J. M., Höpfner M., Morris, P. E., Raspollini, P., Stiller, G., and Wells, R. J.: Optimized forward model and retrieval scheme for MIPAS near-real-time data processing, Appl. Optics, 39, 1323–1340, 2000. 7702, 7705, 7709

Schwärz M., Kirchengast, G., Leuprecht, A., Fritzer, A., Scherllin-Pirscher, B., and Retscher, C.: Validating Satellite Observations of Thermodynamic Variables by Reference Datasets from GPS Radio Occultation, Geophys. Res. Abstr., 14, EGU2012-12647, 2012, EGU General Assembly, 2012. 7706

Stiller, G.: The Karlsruhe Optimized and Precise Radiative Transfer Algorithm, Institut für Meteorologie und Klimaforschung, 2000. 7704

AMTD

7, 7701–7715, 2014

Thayer, G. D.: A rapid and accurate ray tracing algorithm for a horizontally stratified atmosphere, Radio Sci., 1, 249–252, 1967. 7704
US Standard Atmosphere, 1976, US Government Printing Office, Washington DC, 1976. 7706
Young, A. T.: Refractivity of air, available at: http://mintaka.sdsu.edu/GF/explain/atmos_refr/air_refr.html (last access: 24 July 2014), 2011. 7705

AMTD
7, 7701–7715, 2014

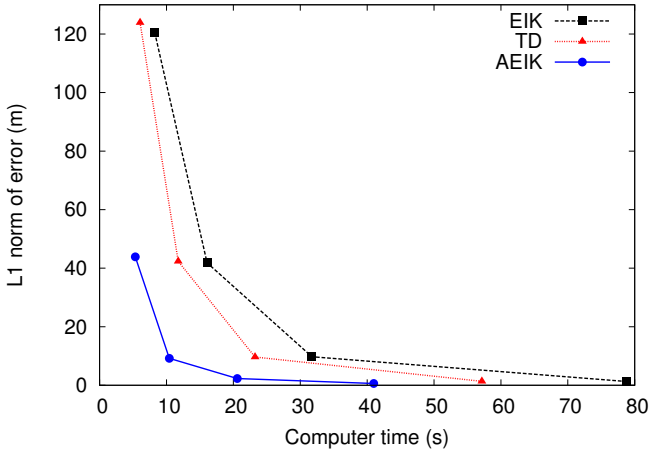

Figure 1. Efficiency of the tested ray-tracing methods, for step sizes of 0.1, 0.25, 0.5 and 1.0 km.

AMTD
7, 7701–7715, 2014

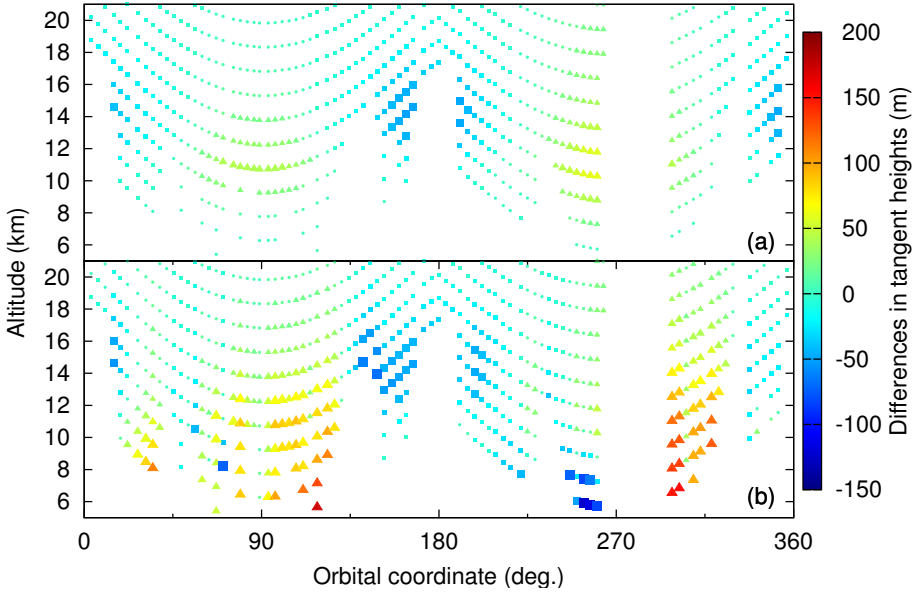

Figure 2. Differences between recalculated and original tangent heights. Assumed atmospheres: IG2 **(a)**, retrieved atmosphere **(b)**. Larger points indicate larger positive (triangles) or negative (squares) differences.

AMTD
7, 7701–7715, 2014

Characterization of the tangent height errors

M. Ridolfi and L. Sgheri

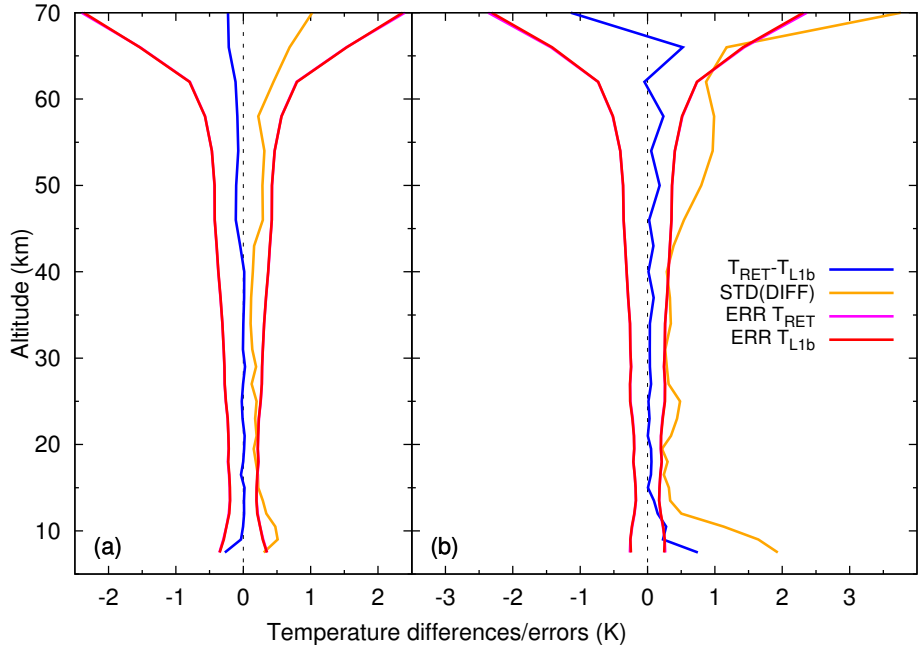

Figure 3. Average difference between temperature retrieved with recalculated (T_{RET}) and original (T_{L1b}) tangent heights, and standard deviation of the differences. Error profiles of T_{RET} and T_{L1b}. Standard **(a)** and constant tangent pressures **(b)** retrieval cases.

AMTD
7, 7701–7715, 2014